

# Anomalous integer quantum Hall effect in AA-stacked bilayer graphene

Ya-Fen Hsu<sup>1</sup> and Guang-Yu Guo<sup>2,1,\*</sup>

<sup>1</sup>*Department of Physics and Center for Theoretical Sciences,  
National Taiwan University, Taipei 106, Taiwan*

<sup>2</sup>*Graduate Institute of Applied Physics, National Chengchi University, Taipei 116, Taiwan*

(Dated: October 30, 2018)

Recent experiments indicate that AA-stacked bilayer graphenes (BLG) could exist. Since the energy bands of the AA-stacked BLG are different from both the monolayer and AB-stacked bilayer graphenes, different integer quantum Hall effect in the AA-stacked graphene is expected. We have therefore calculated the quantized Hall conductivity  $\sigma_{xy}$  and also longitudinal conductivity  $\sigma_{xx}$  of the AA-stacked BLG within the linear response Kubo formalism. Interestingly, we find that the AA-stacked BLG could exhibit both conventional insulating behavior (the  $\bar{\nu} = 0$  plateau) and chirality for  $|\bar{\mu}| < t$ , where  $\bar{\nu}$  is the filling factor ( $\bar{\nu} = \sigma_{xy}h/e^2$ ),  $\bar{\mu}$  is the chemical potential, and  $t$  is the interlayer hopping energy, in striking contrast to the monolayer graphene (MLG) and AB-stacked BLG. We also find that for  $|\bar{\mu}| \neq [(\sqrt{n_2} + \sqrt{n_1})/(\sqrt{n_2} - \sqrt{n_1})]t$ , where  $n_1 = 1, 2, 3, \dots$ ,  $n_2 = 2, 3, 4, \dots$  and  $n_2 > n_1$ , the Hall conductivity is quantized as  $\sigma_{xy} = \pm \frac{4e^2}{h}n$ ,  $n = 0, 1, 2, \dots$ , if  $|\bar{\mu}| < t$  and  $\sigma_{xy} = \pm \frac{4e^2}{h}n$ ,  $n = 1, 2, 3, \dots$ , if  $|\bar{\mu}| > t$ . However, if  $|\bar{\mu}| = [(\sqrt{n_1} + \sqrt{n_2})/(\sqrt{n_2} - \sqrt{n_1})]t$ , the  $\bar{\nu} = \pm 4(n_1 + n_2)n$  plateaus are absent, where  $n = 1, 2, 3, \dots$ , in comparison with the AB-stacked BLG within the two-band approximation. We show that in the low-disorder and high-magnetic-field regime,  $\sigma_{xx} \rightarrow 0$  as long as the Fermi level is not close to a Dirac point, where  $\Gamma$  denotes the Landau level broadening induced by disorder. Furthermore, when  $\sigma_{xy}$  is plotted as a function of  $\bar{\mu}$ , a  $\bar{\nu} = 0$  plateau appears across  $\bar{\mu} = 0$  and it would disappear if the magnetic field  $B = \pi t^2 / N e h v_F^2$ ,  $N = 1, 2, 3, \dots$ . Finally, the disappearance of the zero-Hall conductivity plateau is always accompanied by the occurrence of a  $8e^2/h$ -step at  $\bar{\mu} = t$ .

PACS numbers: 73.43.Cd, 71.70.Di, 72.80.Vp, 73.22.Pr

## I. INTRODUCTION

Graphene exhibits many peculiar properties[1] and has greatly intrigued physicists in recent years. Charge carriers in the monolayer graphene (MLG) possess a linear energy dispersion (see Fig. 1a)[2] and are of chiral nature[3] near each Dirac point. The quasiparticles in the AB-stacked bilayer graphene (BLG) are also chiral. However, unlike MLG, the energy spectra of the AB-stacked BLG are parabolic (Fig. 1b). One of the interesting properties of graphene is quantum Hall effect (QHE). Indeed, both theoretical[4] and experimental works[5–7] show that integer quantum Hall effect (IQHE) in MLG is unconventional. The Hall conductivity in MLG is quantized as  $\sigma_{xy} = \pm \frac{4e^2}{h}(n + \frac{1}{2})$ , where  $n = 0, 1, 2, \dots$ . The factor 4 comes from the fourfold (spin and valley) degeneracy. Furthermore, because the states are shared by electron and hole at the zeroth Landau level (LL), the shift of  $1/2$  occurs. In contrast, in the AB-stacked BLG, within the two-band parabolic approximation, the Hall conductivity was shown to be  $\sigma_{xy} = \pm \frac{4e^2}{h}n$ , where  $n = 1, 2, 3, \dots$ [8]. The zeroth and first Landau levels are degenerate and hence the first quantum Hall plateau appears at  $4e^2/h$  instead of  $2e^2/h$ . This phenomenon has been observed experimentally[9]. QHE of the AB-stacked BLG was also studied based on a four-band Hamiltonian in Ref. [10].

Although AB stacking is predicted to be energetically favored over AA stacking in *ab initio* density functional theory (DFT) calculations, the energy difference of about 0.02 eV/cell is small[11, 12]. Moreover, Lauffer *et al.* found that scanning tunneling microscopy (STM) images of BLG resemble that of MLG, and hence they regarded it as a consequence of the BLG configuration being close to AA stacking[13]. Moreover, Liu *et al.* reported that in their high-resolution transmission electron microscope (HR-TEM) experiments a high proportion of thermally treated samples are AA-stacked BLG[14]. These findings indicate the possibility of fabrication of the AA-stacked BLG. Since the energy bands of the AA-stacked BLG (see Fig. 1c) are different from both the AB-stacked BLG and monolayer graphene, the quantum Hall effect in the AA-stacked is expected to be quite different from that in the latter two systems.

We have therefore carried out a theoretical study of IQHE as well as the longitudinal conductivity  $\sigma_{xx}$  in the AA-stacked bilayer graphene using the Kubo formalism. In this paper, we present a general analytical form of the Hall conductivity  $[\sigma_{xy}(\bar{\mu}, B)]$  as a function of both chemical potential ( $\bar{\mu}$ ) and magnetic field ( $B$ ) of the AA-stacked BLG. Our presentation will be divided into two parts: i) the variation of the  $\sigma_{xy}$  vs.  $1/B$  curve with some fixed  $\bar{\mu}$ 's and ii) the effect of the magnetic field on the  $\sigma_{xy}$  vs.  $\bar{\mu}$  curve. Our main findings are as follows. Firstly, for  $|\bar{\mu}| \neq [(\sqrt{n_2} + \sqrt{n_1})/(\sqrt{n_2} - \sqrt{n_1})]t$ , where  $t$  is the interlayer hopping energy,  $n_1$  and  $n_2$  are any integers larger than 1 and 2, respectively, and  $n_1 < n_2$ , the Hall

\*Electronic address: gyguo@phys.ntu.edu.tw

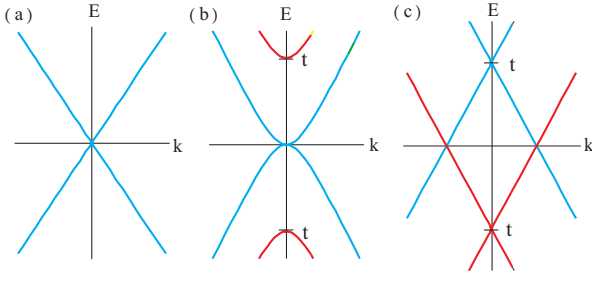


FIG. 1: (color online) The energy bands of (a) monolayer graphene, (b) AB-stacked bilayer graphene, and (c) AA-stacked bilayer graphene.

conductivity is quantized as

$$\begin{aligned} \sigma_{xy} &= \pm \frac{4e^2}{h} n, \quad n = 0, 1, 2, \dots, \quad \text{if } |\bar{\mu}| < t \\ \sigma_{xy} &= \pm \frac{4e^2}{h} n, \quad n = 1, 2, 3, \dots, \quad \text{if } |\bar{\mu}| > t. \end{aligned} \quad (1)$$

However, if  $|\bar{\mu}| = [(\sqrt{n_2} + \sqrt{n_1})/(\sqrt{n_2} - \sqrt{n_1})]t$ , the Hall conductivity is given by

$$\sigma_{xy} = \pm \frac{4e^2}{h} n, \quad \text{excluding } \pm \frac{4e^2}{h} (n_1 + n_2)n, \quad n = 1, 2, 3, \dots \quad (2)$$

Secondly, in the low-disorder and high-magnetic-field regime [ $\Gamma \rightarrow 0$  and  $\hbar^4 \omega_c^4 \gg (\bar{\mu} + \nu t)^4$ ],  $\sigma_{xx} \approx (8e^2/\pi h)[(\bar{\mu}^2 + t^2)\Gamma^2/(\bar{\mu}^2 - t^2)^2 + 2\Gamma^2/\hbar^2 \omega_c^2 + 5(\bar{\mu}^2 + t^2)\Gamma^2/\hbar^4 \omega_c^4] \rightarrow 0$  if the Fermi level is not close to a Dirac point, where  $\hbar\omega_c$  is the cyclotron energy. That is to say, if the magnetic field is high enough, the applied electric field cannot drive any current for  $|\bar{\mu}| < t$ , while the current is perpendicular to external electric field for  $|\bar{\mu}| > t$ . Thirdly, we find that the  $\sigma_{xy} = 0$  (the filling factor  $\bar{\nu} = 0$ ) plateau across  $\bar{\mu} = 0$  would disappear when  $B = \pi t^2 / N e \hbar v_F^2$ ,  $N = 1, 2, 3, \dots$ , and that a  $8e^2/h$ -step at  $\bar{\mu} = t$  occurs while a zero-Hall conductivity plateau disappears. Interestingly, unlike the monolayer and AB-stacked bilayer graphenes, the AA-stacked bilayer graphene could display a unusual  $\bar{\nu} = 0$  plateau even though it contains chiral quasiparticles. We argue that the occurrence of the  $\bar{\nu} = 0$  plateau is due to the shift of level anomalies by the interlayer hopping energy  $t$ .

## II. THEORETICAL MODEL AND ANALYTICAL CALCULATION

### A. Model Hamiltonian and Landau levels

We first derive an effective four-band Hamiltonian near each Dirac point for the AA-stacked bilayer graphene in tight-binding approximation via  $\mathbf{k} \cdot \mathbf{p}$  expansion[1]. We then diagonalize this Hamiltonian to obtain the energy bands of the AA-stacked BLG. In Fig. 1, we display the

energy bands of the MLG, AB-stacked, and AA-stacked BLG together. We find that the energy bands of the AA-stacked BLG are just two copies of the MLG band structure shifted up and down by  $t$ , respectively. Hence,  $E = \pm t$  are the Dirac points for the AA-stacked BLG. When a magnetic field is applied, we should replace the momentum operator  $\mathbf{p}$  with  $\mathbf{p} + e\mathbf{A}/c$ , where the external magnetic field  $\mathbf{B} = \nabla \times \mathbf{A}$  and  $-e$  is the charge of an electron. The magnetic field is applied along the positive  $z$ -axis (i.e. out of plane) and hence the vector potential can be written as  $\mathbf{A} = (-By, 0, 0)$  in the Landau gauge. Therefore, the effective four-band Hamiltonian in the presence of the magnetic field is given by

$$\begin{aligned} H_{\pm} &= \begin{pmatrix} v_F(\sigma_x \pi_x \pm \sigma_y \pi_y) & -tI \\ -tI & v_F(\sigma_x \pi_x \pm \sigma_y \pi_y) \end{pmatrix} \\ &: \begin{cases} \pi_x = -i\hbar\partial_x - eBy/c, \\ \pi_y = -i\hbar\partial_y. \end{cases} \end{aligned} \quad (3)$$

Here  $\pm$  label the two valleys of the band structure at  $K$  and  $K'$ , respectively.  $v_F$  denotes the Fermi velocity. In the Landau gauge, we can substitute the eigenfunction  $\psi = e^{ikx}\phi(y)$  of the Hamiltonian into the Schrödinger equation  $H\psi = E\psi$ . Here  $\phi(y)$  can be written as  $(\phi_1(y), \phi_2(y))^T$ , where  $\phi_1$  and  $\phi_2$  are two-component column vectors. Then, we make the transformations:  $\sigma^{\pm} = \sigma_x \pm i\sigma_y$ ,  $\xi = y/\ell_B - \ell_B k$  and  $O^{\mp} = (\xi \pm \partial_{\xi})/\sqrt{2}$ , where the magnetic length  $\ell_B = \sqrt{\hbar c/|eB|}$ . Finally, for the  $K$  valley, the Schrödinger equation reads

$$\begin{aligned} \begin{pmatrix} \frac{-\hbar v_F}{\sqrt{2}\ell_B}(O^{-}\sigma^{+} + O^{+}\sigma^{-}) & -tI \\ -tI & \frac{\hbar v_F}{\sqrt{2}\ell_B}(O^{-}\sigma^{+} + O^{+}\sigma^{-}) \end{pmatrix} \begin{pmatrix} \phi_1 \\ \phi_2 \end{pmatrix} \\ = E \begin{pmatrix} \phi_1 \\ \phi_2 \end{pmatrix}. \end{aligned} \quad (4)$$

Since  $O^{\mp}$  satisfy the commutation relation:  $[O^{-}, O^{+}] = 1$ ,  $O^{\mp}$  are the annihilation and creation operators of one-dimensional (1-D) simple harmonic oscillator (SHO), respectively. Similarly,  $\sigma^{\pm}$  are the raising and lowering operators of pseudospin angular momentum. Obviously, the eigenstates of  $O^{-}\sigma^{+} + O^{+}\sigma^{-}$  are  $(|N-1\rangle, \pm|N\rangle)^T$  if  $N \geq 1$  and  $(0, |0\rangle)^T$  if  $N = 0$ , where  $|N\rangle$  are the eigenstates of the 1-D SHO. All non-zero vectors are eigenvectors of  $-tI$ . Therefore, we can infer that the eigenvalues of Eq. (4) are

$$E_N^{\mu\nu} = -\mu\sqrt{N}\hbar\omega_c - \nu t \quad (5)$$

with  $\omega_c = \sqrt{2}v_F/\ell_B$  and the eigenstates of Eq. (4) are

$$\begin{cases} |0, +, \nu\rangle = \frac{1}{\sqrt{2}} \begin{pmatrix} 0 \\ |0\rangle \\ 0 \\ \nu|0\rangle \end{pmatrix}, & \text{if } N = 0, \\ |N, \mu, \nu\rangle = \frac{1}{2} \begin{pmatrix} |N-1\rangle \\ \mu|N\rangle \\ \nu|N-1\rangle \\ \mu\nu|N\rangle \end{pmatrix}, & \text{if } N \geq 1, \end{cases} \quad (6)$$

Here the indice  $\mu = \pm$  and  $\nu = \pm$ . Clearly, the LLs of the AA-stacked BLG are just two copies of the LLs of the MLG shifted up and down by  $t$ , respectively.

### B. Linear response calculation

The conductivity can be calculated using the Kubo formula within the linear response theory[15]. The Kubo formula for the DC-conductivity is given by

$$\sigma_{ij} = \lim_{\Omega \rightarrow 0} \frac{\text{Im}\Pi_{ij}^R(\Omega + i0)}{\hbar\Omega}. \quad (7)$$

Here the retarded current-current correlation  $\Pi_{ij}^R$  in the Matsubara form reads[10]

$$\Pi_{ij}^R(i\nu_m) = -\frac{4e^2}{2\pi\ell_B^2\beta\hbar} \times \sum_{n=-\infty}^{\infty} \sum_{k,\ell=0}^{\infty} \sum_{\substack{\mu,\rho \\ \pm}} \sum_{\substack{\nu,\sigma \\ \pm}} \frac{\langle k, \mu, \nu | v_i | \ell, \rho, \sigma \rangle \langle \ell, \rho, \sigma | v_j | k, \mu, \nu \rangle}{(i\tilde{\omega}_n - \tilde{E}_k^{\mu\nu})(i\tilde{\omega}_n + i\nu_m - \tilde{E}_\ell^{\rho\sigma})}, \quad (8)$$

where the factor 4 is due to the fourfold (spin and valley) degeneracy, the velocity operator  $v_i = [x_i H_+]/i\hbar$ , and  $\tilde{E}_k^{\mu\nu} = E_k^{\mu\nu}/\hbar$ .  $\omega_n$  and  $\nu_m$  are Matsubara frequencies of fermion and boson, respectively. When the chemical potential and disorder scattering are considered, Matsubara frequency of fermion has to be corrected as  $i\tilde{\omega}_n = i\omega_n + \bar{\mu}/\hbar + i\text{sgn}(\omega_n)\Gamma/\hbar$ .  $\Gamma$  is the Landau level broadening due to the presence of disorder. Substituting the eigenstates of  $H_+$  into Eq. (8), we obtain

$$\Pi_{xy}^R(i\nu_m) = -\frac{ie^2v_F^2}{2\pi\ell_B^2\beta\hbar} \left( 2 \sum_{\substack{\mu,\nu \\ \pm}} \chi_{1,0}^{\mu\nu,\nu} + \sum_{\ell \geq 1} \sum_{\substack{\mu,\rho \\ \pm}} \sum_{\nu=\pm} \chi_{\ell+1,\ell}^{\mu\nu,\rho\nu} \right), \quad (9)$$

where  $\chi_{k,\ell}^{\mu\nu,\rho\sigma}$  is defined as

$$\chi_{k,\ell}^{\mu\nu,\rho\sigma}(i\nu_m) = \sum_{n=-\infty}^{n=\infty} \left[ \frac{1}{(i\tilde{\omega}_n - \tilde{E}_k^{\mu\nu})(i\tilde{\omega}_n + i\nu_m - \tilde{E}_\ell^{\rho\sigma})} - (i\nu_m \rightarrow -i\nu_m) \right]. \quad (10)$$

In the DC and clean limit, we let  $\Omega + i0 \rightarrow 0$  and set  $\Gamma = 0$ . Then, after evaluating the Matsubara sums[15], we find that

$$\frac{1}{\beta\hbar} \chi_{k,\ell}^{\mu\nu,\rho\sigma} |_{i\nu_m=\Omega+i0 \rightarrow 0} \approx \frac{-2(\Omega + i0)[f(E_k^{\mu\nu}) - f(E_\ell^{\rho\sigma})]}{(\tilde{E}_k^{\mu\nu} - \tilde{E}_\ell^{\rho\sigma})^2}, \quad (11)$$

where  $f(E)$  is the Fermi-Dirac distribution. Furthermore, we define  $\tilde{f}(E) = f(E) - 1/2$ . Then, using Eqs. (7), (9) and (11) and considering the variation of direction of conductivity with the signs of magnet field and carrier charge, we can derive that

$$\sigma_{xy} = -\frac{4e^2}{h} \text{sgn}(eB) \left[ \sum_{\nu=\pm} \tilde{f}(E_0^{+\nu}) + \sum_{\ell \geq 1} \sum_{\substack{\mu,\nu \\ \pm}} \tilde{f}(E_\ell^{\mu\nu}) \right] \quad (12)$$

At zero temperature,  $f(E) = 1$  and  $f(E) = 0$  for the occupied and unoccupied LLs, respectively. The LLs located at  $E \leq \bar{\mu}$  are occupied and the others are empty. That is to say,  $\tilde{f}(E) = 1/2$  for  $E \leq \bar{\mu}$ , while  $\tilde{f}(E) = -1/2$  for  $E > \bar{\mu}$ . Therefore, we only need to calculate the number of LLs between  $-\bar{\mu}$  and  $\bar{\mu}$  to determine the magnitude of the Hall conductivity. Moreover, for  $-|\bar{\mu}| < E < |\bar{\mu}|$ , the number of the up-shifted LLs ( $\nu = -$ ) is equal to that of the down-shifted LLs ( $\nu = +$ ). Hence, we find that the zero-temperature Hall conductivity is given by

$$\sigma_{xy} = -\frac{4e^2}{h} \text{sgn}(\bar{\mu}) \text{sgn}(eB) [\theta(|\bar{\mu}| + t)\theta(|\bar{\mu}| - t) + \sum_{\ell \geq 1} \sum_{\mu=\pm} \theta(|\bar{\mu}| - E_\ell^{\mu-})\theta(|\bar{\mu}| + E_\ell^{\mu-})]. \quad (13)$$

Eq. (13) indicates that the Hall conductivity would simply change its sign as  $\bar{\mu} \rightarrow -\bar{\mu}$  and that the Hall conductivity is equal to  $4e^2/h$  times the number of up-shifted LLs between  $-|\bar{\mu}|$  and  $|\bar{\mu}|$ . Eq. (13) can also be written in the form

$$\sigma_{xy} = -\frac{4e^2}{h} \text{sgn}(\bar{\mu}) \text{sgn}(eB) \times \left\{ \theta(|\bar{\mu}| - t - \sqrt{2\hbar v_F^2 |eB|/c}) \left[ \frac{c(|\bar{\mu}| - t)^2}{2\hbar v_F^2 |eB|} \right] + \theta(\sqrt{2\hbar v_F^2 |eB|/c} - t + |\bar{\mu}|) \left[ \frac{c(|\bar{\mu}| - t)^2}{2\hbar v_F^2 |eB|} \right] + \left[ \frac{c(|\bar{\mu}| + t)^2}{2\hbar v_F^2 |eB|} \right] - \left[ \frac{c(|\bar{\mu}| - t)^2}{2\hbar v_F^2 |eB|} \right] + \theta(|\bar{\mu}| + t)\theta(|\bar{\mu}| - t) \right\}. \quad (14)$$

Here  $[x]$  means the integer part of  $x$ . The last term is the contribution of level anomalies ( $N = 0$ )[4].

We also calculate the longitudinal conductivity ( $\sigma_{xx}$ ) via the Kubo formula. The longitudinal conductivity have to be evaluated under the effect of disorder scattering ( $\Gamma \neq 0$ ). Using Cauchy's integral theorem as in Refs. [16, 17], we can obtain

$$\sigma_{xx} = \frac{e^2}{\pi\hbar} \omega_c^2 \left\{ \int_{-\infty}^{\infty} dE \left( -\frac{\partial f}{\partial E} \right) \times \left[ \sum_{\substack{\mu,\rho \\ \pm}} \sum_{\nu=\pm} \sum_{\ell \geq 1} \text{Im}\tilde{g}_{\ell+1}^{\mu\nu}(E) \text{Im}\tilde{g}_\ell^{\rho\nu}(E) + 2 \sum_{\substack{\mu,\nu \\ \pm}} \text{Im}\tilde{g}_1^{\mu\nu}(E) \text{Im}\tilde{g}_0^{+\nu}(E) \right] \right\}, \quad (15)$$

where  $\tilde{g}_\ell^\rho = 1/(E/\hbar - \tilde{E}_\ell^{\rho\nu} + i\Gamma/\hbar)$ . Applying the techniques of partial-fraction decomposition similar to that used in Ref. [18] and after some cumbersome algebra, we finally find that the zero-temperature longitudinal conductivity can be written in terms of the digamma func-

tion ( $\varphi_0$ )[19],

$$\begin{aligned}
\sigma_{xx} = & \frac{4e^2}{\pi h} \sum_{\nu=\pm} \left\{ i \left[ \varphi_0 \left( -\frac{(\bar{\mu} + \nu t)^2 - \Gamma^2}{\hbar^2 \omega_c^2} + 1 - i \frac{2\Gamma(\bar{\mu} + \nu t)}{\hbar^2 \omega_c^2} \right) \right. \right. \\
& - \left. \varphi_0 \left( -\frac{(\bar{\mu} + \nu t)^2 - \Gamma^2}{\hbar^2 \omega_c^2} + 1 + i \frac{2\Gamma(\bar{\mu} + \nu t)}{\hbar^2 \omega_c^2} \right) \right] \\
& \times \frac{[2(\bar{\mu} + \nu t)^3 \Gamma + 2(\bar{\mu} + \nu t) \Gamma^3]}{p} \\
& + \frac{[\hbar^6 \omega_c^6 + \hbar^4 \omega_c^4 (\bar{\mu} + \nu t)^2 - 12 \hbar^2 \omega_c^2 (\bar{\mu} + \nu t)^4 + 8(\bar{\mu} + \nu t)^6] \Gamma^2}{q} \\
& + \frac{[\hbar^4 \omega_c^4 + 4 \hbar^2 \omega_c^2 (\bar{\mu} + \nu t)^2 + 16(\bar{\mu} + \nu t)^4] \Gamma^4}{q} \\
& + \frac{8(\bar{\mu} + \nu t)^2 \Gamma^6}{q} \\
& + \frac{[\hbar^2 \omega_c^2 (\bar{\mu} + \nu t)^2 + \hbar^4 \omega_c^4] \Gamma^2 + \hbar^2 \omega_c^2 \Gamma^4}{[(\bar{\mu} + \hbar \omega_c + \nu t)^2 + \Gamma^2][(\bar{\mu} - \hbar \omega_c + \nu t)^2 + \Gamma^2]} \\
& \left. \times \frac{1}{(\bar{\mu} + \nu t)^2 + \Gamma^2} \right\}. \tag{16}
\end{aligned}$$

Here,

$$\begin{aligned}
p &= \hbar^4 \omega_c^4 + 16 \Gamma^2 (\bar{\mu} + \nu t)^2, \\
q &= \{ [(\bar{\mu} + \nu t)^2 - \hbar^2 \omega_c^2 - \Gamma^2]^2 + 4 \Gamma^2 (\bar{\mu} + \nu t)^2 \} \times p. \tag{17}
\end{aligned}$$

Unlike Ref. 20, we do not adopt low-magnetic field approximation here and therefore Eq. (16) is general and suitable for all values of the applied magnetic field. However, when we adopt the low-disorder and high-magnetic-field limit, we first consider  $\Gamma$  as being small and keep the terms in the order of  $\Gamma^2$ . Then, we let  $(\bar{\mu} + \nu t)/(\hbar^4 \omega_c^4) \rightarrow 0$ , Eq. (16) could be simplified as

$$\sigma_{xx} \approx \frac{4e^2}{\pi h} \left[ \frac{(\bar{\mu}^2 + t^2) \Gamma^2}{(\bar{\mu}^2 - t^2)^2} + 2 \frac{\Gamma^2}{\hbar^2 \omega_c^2} + 5 \frac{\bar{\mu}^2 + t^2}{\hbar^2 \omega_c^2} \frac{\Gamma^2}{\hbar^2 \omega_c^2} \right]. \tag{18}$$

The first term is independent of  $B$ . The second and third terms are proportional to  $1/B$  and  $1/B^2$ , respectively.

### III. DEPENDENCE OF CONDUCTIVITY ON MAGNETIC FIELD AND CHEMICAL POTENTIAL

Since both the magnetic field and chemical potential could be tuned experimentally, we display the calculated conductivity as a function of  $1/B$  and  $\bar{\mu}$  in this Sec. Here we use the interlayer hopping energy  $t = 0.2$  eV for the AA-stacking and  $t = 0.4$  eV for the AB-stacking as determined by the *ab initio* DFT calculations within the local density approximation (LDA)[21]. Moreover, because the quantized values of the Hall conductivity is independent of the presence of disorder scattering[22], we show only the Hall conductivity in the clean limit (i.e.,  $\Gamma = 0$ ) and analyze the Hall plateaus qualitatively.

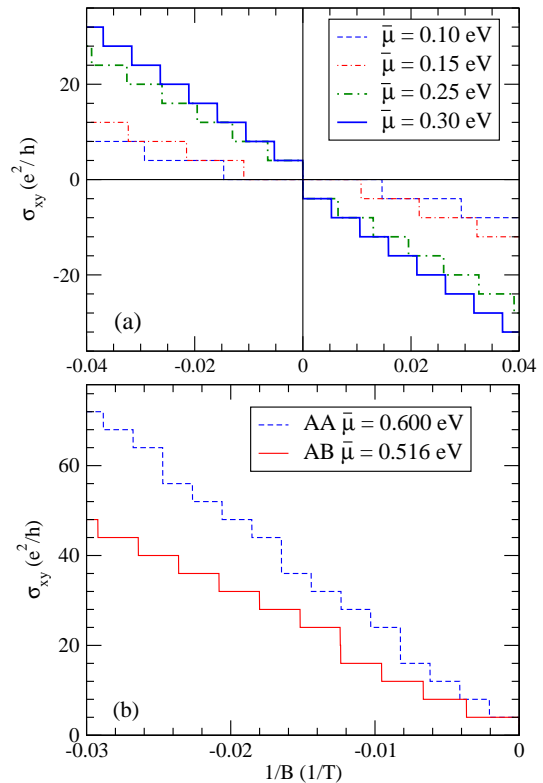


FIG. 2: (color online) (a) The quantized Hall conductivity  $\sigma_{xy}$  of the AA-stacked bilayer graphene as a function of  $1/B$  for several values of chemical potential  $\bar{\mu}$ . (b) The quantized Hall conductivity  $\sigma_{xy}$  of both AA-stacked and AB-stacked bilayer graphenes as a function of  $1/B$ . The interlayer hopping energy  $t$  used is 0.2 eV for the AA-stacking and 0.4 eV for the AB-stacking, and  $v_F = 1.0 \times 10^6$  m/s. The Hall conductivity  $\sigma_{xy}$  for the AB-stacking was obtained by using Eq. 15 from Ref. 10.

#### A. Conductivities vs inverse of magnetic field

In Fig. 2, the Hall conductivity is plotted as a function of  $1/B$  and we should discuss the effect of chemical potential on the  $\sigma_{xy}$  vs.  $1/B$  curve. From Fig. 2(a), we see that  $\sigma_{xy} = \pm \frac{4e^2}{h} n$ , with  $n = 0, 1, 2, \dots$ , for  $|\bar{\mu}| < t$ , and  $n = 1, 2, 3, \dots$ , for  $|\bar{\mu}| > t$ , excluding  $|\bar{\mu}| = [(\sqrt{n_2} + \sqrt{n_1})/(\sqrt{n_2} - \sqrt{n_1})]t$ , where  $n_1 = 1, 2, 3, \dots$  and  $n_2 = 2, 3, 4, \dots$ . It is clear from either Eq. (13) or Eq. (14) that  $\sigma_{xy}(-\bar{\mu}) = -\sigma_{xy}(\bar{\mu})$ , and hence we did not show any curves for  $\bar{\mu} < 0$  in Fig. 2(a). Interestingly, in contrast to the MLG and AB-stacked BLG, the AA-stacked BLG displays the pronounced  $\bar{\nu} = 0$  plateau for  $|\bar{\mu}| < t$ , where the filling factor  $\bar{\nu} = \sigma_{xy} h / e^2$ . The MLG and AB-stacked BLG lack the  $\bar{\nu} = 0$  plateau because their level anomalies are located at  $E = 0$ . The level anomaly of the MLG is the zeroth Landau level while those of the AB-stacked BLG are the zeroth and first Landau levels. The occurrence of level anomalies is a remarkable manifestation of the unique property of chiral quasiparticles[8, 23]. In the AA-stacked BLG, similarly, level anomalies also

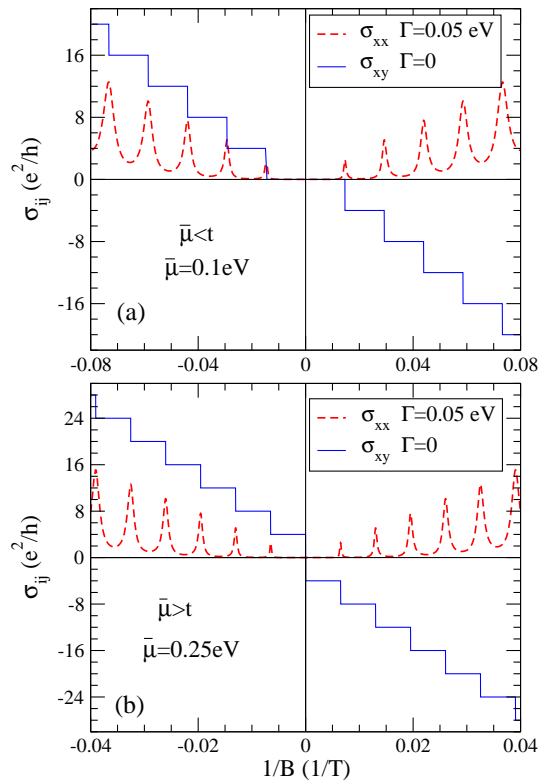


FIG. 3: (color online) The longitudinal ( $\sigma_{xx}$ ) and transverse ( $\sigma_{xy}$ ) conductivities of the AA-stacked bilayer graphene as a function of  $1/B$ , (a) for  $|\bar{\mu}| < t$ , and (b) for  $|\bar{\mu}| > t$ . The rest parameters are the same as in Fig. 2.

exist in the LL spectrum. However, for the AA-stacked BLG, the level anomalies are shifted up and down by  $t$ , respectively. Thus, these level anomalies are unique in the sense that they are always located at the Dirac points regardless of the magnitude of  $B$ , in contrast with the other Landau levels[4, 8, 10]. It is worth mentioning that the Dirac points often exhibit interesting electronic properties, such as electron-hole puddle formation[24, 25], and Andreev reflection type transitions.[26] Until now, some transport properties at these Dirac points remain to be understood[27]. The level anomaly is one of the interesting properties of the Dirac points and recently the nature of its electronic states (being metallic or insulating) in the high magnetic field-low temperature regime is hotly debated[28].

Displayed in Fig. 2(b) are the Hall plateaus of the AA-stacked BLG for  $|\bar{\mu}| = [(\sqrt{n_2} + \sqrt{n_1})/(\sqrt{n_2} - \sqrt{n_1})]t$ . We find that in addition to the  $\bar{\nu} = 0$  plateau, other differences between the AA-stacked and AB-stacked BLGs exist. In particular, when  $|\bar{\mu}| = [(\sqrt{n_2} + \sqrt{n_1})/(\sqrt{n_2} - \sqrt{n_1})]t$ , some  $8e^2/h$ -steps appear at  $1/B \neq 0$ . In other words, in comparison with the other cases of  $|\bar{\mu}| > t$  ( $|\bar{\mu}| \neq [(\sqrt{n_1} + \sqrt{n_2})/(\sqrt{n_2} - \sqrt{n_1})]$ ), some plateaus would be missing for  $|\bar{\mu}| = [(\sqrt{n_2} + \sqrt{n_1})/(\sqrt{n_2} - \sqrt{n_1})]t$ . Furthermore, these  $8e^2/h$ -steps appear periodically. Taking  $\bar{\mu} = 3t$  (i.e.  $n_2 = 4, n_1 = 1$ ), for example, between any

two  $8e^2/h$ -steps, the curve passes through three  $4e^2/h$ -steps and four plateaus. Only the Hall plateaus  $\sigma_{xy} = \frac{4e^2}{h}n$ ,  $n = \pm 1, \pm 2, \pm 3, \pm 4, \pm 6, \pm 7, \pm 8, \pm 9, \pm 11, \pm 12, \dots$ , appear. In other words, the Hall plateaus  $n = \pm 5, \pm 10, \pm 15, \dots$  are absent here. When  $|\bar{\mu}| > t$ , the quantum Hall effect of the AB-stacked BLG must be studied based on a four-band Hamiltonian[10]. Based on the four-band model[10], for  $|\bar{\mu}| > t$ , the AB-stacked BLG can also exhibit a  $8e^2/h$ -step, as shown in Fig. 2(b). Although the  $8e^2/h$ -step is not specific to the AA-stacked BLG, the periodic appearance of the  $8e^2/h$ -steps has never been seen in the AB-stacked BLG and hence is a unique characteristic of the AA-stacked BLG.

The longitudinal and transverse conductivities as a function of  $1/B$  are plotted together in Fig. 3. It is seen from Fig. 3 that the longitudinal conductivity goes to a local minima at the position of the Hall plateaus and reaches a local maxima as the steps appear except the step at  $1/B = 0$ . The unique  $\bar{\nu} = 0$  Hall plateau of the AA-stacked bilayer graphene for  $|\bar{\mu}| < t$  is especially interesting. From Fig. 3(a), we find that  $\sigma_{xx}$  falls to zero as the  $\bar{\nu} = 0$  Hall plateau emerges. As stated previously, for  $|\bar{\mu}| > t$ , the AA-stacked BLG lacks the  $\bar{\nu} = 0$  Hall plateau. The first Hall plateau occurs at  $\bar{\nu} = 4$  or  $\bar{\nu} = -4$ . This encourages us to investigate the difference between the longitudinal conductivities at the  $\bar{\nu} = 0$  Hall plateau for  $|\bar{\mu}| < t$  and at the  $\bar{\nu} = \pm 4$  Hall plateaus for  $|\bar{\mu}| > t$ . Fig. 3(b) shows that for  $|\bar{\mu}| > t$ , the  $\sigma_{xx}$  goes to zero as the first Hall plateau occurs. This implies that at the high magnetic field, the external electric field cannot drive any current for  $|\bar{\mu}| < t$  while the current is perpendicular to the external electric field for  $|\bar{\mu}| > t$ . Here  $\bar{\mu}$  and  $t$  are in the order of 0.1 eV while the order of magnitude of  $\Gamma$  [ $\mathcal{O}(\Gamma)$ ] is 0.01 eV.  $\bar{\mu} + \nu t$  are about one order of magnitude higher than  $\Gamma$  ( $\bar{\mu} + \nu t \sim 10\Gamma$ ). Therefore, the condition of low disorder is satisfied. If  $\hbar^4\omega_c^4 \gg (\bar{\mu} + \nu t)$ , Eq. (18) can be applied here. This needs  $\hbar\omega_c$  to be larger than 1.78 ( $\bar{\mu} + \nu t$ ) and  $B$  is estimated to be at least a few times larger than 10 T. In the low-disorder and high-magnetic-field regime, we roughly estimate from Eq. (18)

$$\sigma_{xx} \sim \frac{4e^2}{h} \left[ \frac{2(\bar{\mu}^2 + t^2)\Gamma^2}{\pi(\bar{\mu}^2 - t^2)^2} + \mathcal{O}(0.001) \right]. \quad (19)$$

When  $\mathcal{O}(|\bar{\mu}| - t) \geq 1\Gamma$ ,  $\sigma_{xx} \sim 0.1(4e^2/h) \rightarrow 0$ .

Interestingly, the results shown in Fig. 2 could be explained in terms of Fig. 4. Let us account for Fig. 2(a) first. It is clear from Fig. 4 that for  $|\bar{\mu}| < t$ , level anomalies are outside the range of  $-\bar{\mu} \sim \bar{\mu}$ . Conversely, for  $|\bar{\mu}| > t$ , level anomalies are inside the range of  $-\bar{\mu} \sim \bar{\mu}$ . In the high magnetic field regime, for  $|\bar{\mu}| < t$ , no Landau level exists between  $-\bar{\mu}$  and  $\bar{\mu}$  and hence the AA-stacked BLG displays the conventional insulating behaviour (a  $\bar{\nu} = 0$  Hall plateau) even though it possesses chirality. Such behaviour of the AA-stacked BLG is in stark contrast to the MLG and AB-stacked BLG. However, for  $|\bar{\mu}| > t$ , level anomalies are located between  $-\bar{\mu}$



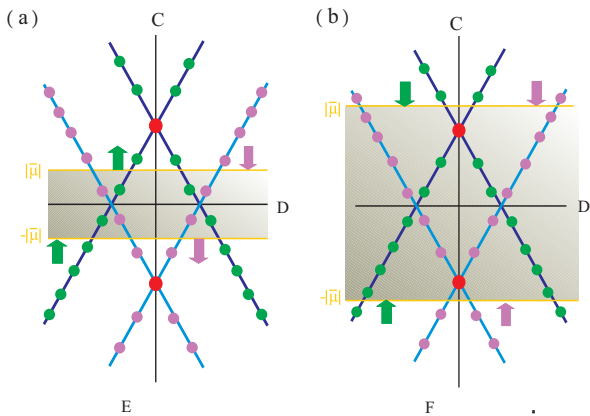


FIG. 4: (color) The Landau level spectrum of the AA-stacked bilayer graphene (a) with  $|\bar{\mu}| < t$  and (b) with  $|\bar{\mu}| > t$ , respectively. Here circles mark the positions of Landau levels. Red, green, and purple circles represent the locations of level anomalies as well as other up-shifted and down-shifted Landau levels, respectively. Mazarine and blue lines denote the up-shifted and down-shifted energy bands, respectively. Shaded is the region between  $-\bar{\mu}$  and  $|\bar{\mu}|$ .

and  $|\bar{\mu}|$  even in the high magnetic field regime and hence a  $\bar{\nu} = 0$  plateau cannot emerge.

The Hall plateaus displayed in Fig. 2(b) can be explained as follows. A up-shifted LL of  $E_k^{-\mu,-}$  and a down-shifted LL of  $E_k^{\mu,+}$  are partners because  $E_k^{\mu,+} = -E_k^{-\mu,-}$ . As the up-shifted LL of  $E_k^{-\mu,-}$  goes through the  $|\bar{\mu}|$ -level, the down-shifted LL of  $E_k^{\mu,+}$  passes through the  $-|\bar{\mu}|$ -level. They always enter the region between  $|\bar{\mu}|$  and  $-|\bar{\mu}|$  (i.e. the shaded region) together and hence each contribute  $4e^2/h$  to the Hall conductivity. Therefore, the Hall conductivity is equal to  $4e^2/h$  times the number of either up-shifted or down-shifted LLs between  $-|\bar{\mu}|$  and  $|\bar{\mu}|$ . Therefore, in order to form a  $8e^2/h$ -step, either two up-shifted or down-shifted LLs must enter or leave the shaded region together. Hence we only need to focus on either up-shifted or down-shifted Dirac cones and discuss the movement of the LLs located in this cone to explain the origin of  $8e^2/h$ -steps. Let us consider the up-shifted Dirac cone. As the magnetic field decreases gradually, the up-shifted LLs would go close to its level anomaly,  $E = t$ . Therefore, we can infer that for  $|\bar{\mu}| < t$ , the LLs above the  $|\bar{\mu}|$ -level (called the upper LLs) go far away from the  $|\bar{\mu}|$ -level, while the LLs below the  $-|\bar{\mu}|$ -level (called the lower LLs) move toward the  $-|\bar{\mu}|$ -level, as shown in Fig. 4(a). The lower LLs would enter the shaded region one by one but the upper LLs can never get into the shaded region. However, for  $|\bar{\mu}| > t$ , both the upper and lower LLs can go close to the shaded region [see Fig. 4(b)], i.e., two up-shifted LLs may enter the shaded region together. Therefore, the  $8e^2/h$ -steps can only appear when  $|\bar{\mu}| > t$ .

For brevity, we use indices  $(k, \mu, \nu)$  to denote the Landau level of  $E_k^{\mu,\nu}$  below. Let us label the two LLs which enter the shaded region together as the  $(k_1, -, -)$  and  $(k_2, +, -)$  LLs. Then,  $k_1/k_2 = (|\bar{\mu}| - t)^2 / (|\bar{\mu}| + t)^2$ .

TABLE I: The characteristics of integer quantum Hall effect in monolayer (ML), AB-stacked bilayer (AB) and AA-stacked bilayer (AA) graphenes as well as conventional two-dimensional semiconductor structures (2D).

	ML	AB	AA	2D
plateau steps ( $\frac{e^2}{h}$ )	4	4, 8 <sup>a</sup>	4, 8 <sup>b</sup>	2
$\bar{\nu} = 0$ plateau	no	no	yes <sup>c</sup>	yes

<sup>a</sup>The  $8\frac{e^2}{h}$  plateau step only occurs (aperiodically) in the four band model (Ref. [10]).

<sup>b</sup>The  $8\frac{e^2}{h}$  plateau step appears periodically for  $|\bar{\mu}| > t$  only.

<sup>c</sup>The  $\bar{\nu} = 0$  plateau occurs only if  $|\bar{\mu}| < t$ .

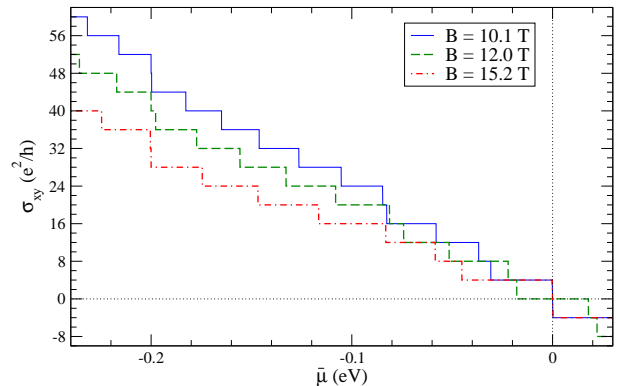


FIG. 5: (color online) The quantized Hall conductivity  $\sigma_{xy}$  of the AA-stacked bilayer graphene as a function of chemical potential  $\bar{\mu}$  for several values of magnetic field  $B$ . The rest parameters are the same as in Fig. 2.

$(n_1, n_2)$  satisfies this condition and  $n_1/n_2$  is an irreducible fraction. Then,  $(k_1, k_2) = (pn_1, pn_2)$ , where  $p = 1, 2, 3, \dots$ , is a set of solutions of  $k_1/k_2 = (|\bar{\mu}| - t)^2 / (|\bar{\mu}| + t)^2$ . Between the entries of  $[(p-1)n_1, (p-1)n_2]$  and  $[pn_1, pn_2]$  LLs,  $(n_1 + n_2 - 2)$  LLs get into the shaded region sequentially as  $1/B$  decreases. Hence,  $(n_1 + n_2 - 2)$   $4e^2/h$ -steps occur between any two  $8e^2/h$ -steps. The Hall conductivity is quantized as  $\sigma_{xy} = \pm \frac{4e^2}{h} n$  with the exception of  $\pm \frac{4e^2}{h} (n_1 + n_2)n$ , where  $n = 1, 2, 3, \dots$ , as shown in Fig. 2(b). Unlike the AB-stacked BLG and the other cases of  $|\bar{\mu}| > t$  of the AA-stacked BLG, the Hall conductivity for  $|\bar{\mu}| = [(\sqrt{n_2} + \sqrt{n_1}) / (\sqrt{n_2} - \sqrt{n_1})]t$  lacks the  $\bar{\nu} = \pm 4(n_1 + n_2)n$  plateaus. Furthermore, it is clear from Fig. 2(b) that when  $|\bar{\mu}| > t$ , the AB-stacked BLG can also exhibit a  $8e^2/h$ -step but the appearance of the  $8e^2/h$ -steps is not periodical. The main findings here are summarized in Table I.

## B. Hall conductivity vs chemical potential

Fig. 5 is a plot of  $\sigma_{xy}$  versus  $\bar{\mu}$ , showing how the Hall plateaus are influenced by the magnetic field. It is clear from Fig. 4 that unlike the MLG and AB-stacked BLG, a  $\bar{\nu} = 0$  plateau centered at  $\bar{\mu} = 0$  appears for  $B = 12$

T in the AA-stacked BLG. However, when the condition of  $\sqrt{2N}\hbar v_F/\ell_B = t$  is reached by tuning the magnetic field, the  $(N, +, -)$  and  $(N, -, +)$  LLs would be located at  $E = 0$ . As a result, the  $\bar{\nu} = 0$  plateau disappears and a  $8e^2/h$ -step at  $\bar{\mu} = 0$  forms, like the AB-stacked BLG. In other words, the absence of the  $\bar{\nu} = 0$  plateau needs the magnetic field  $B = \pi t^2/Ne\hbar v_F^2$ , where  $N = 1, 2, \dots$ . In Fig. 5,  $B = 10.1$  T and  $B = 15.2$  T satisfy this condition with  $N = 3$  and  $N = 2$ , respectively. Thus, these curves lack the  $\bar{\nu} = 0$  plateau.

In addition, we note that a  $8e^2/h$ -step occurs at  $\bar{\nu} = t$  for  $B = 10.1$  T and  $B = 15.2$  T. For  $B = 12$  T, all the LLs are nondegenerate and hence all the steps are of the height of  $4e^2/h$ . However, if the  $(N, -, +)$  and  $(o, +, -)$  LLs are degenerate at  $E = t$ , a  $8e^2/h$ -step appears at  $\bar{\mu} = t$ . This level degeneracy happens as the magnetic field  $B = 4\pi t^2/Ne\hbar v_F^2$ , where  $N = 1, 2, 3, \dots$ .  $B = 10.1$  T and  $B = 15.2$  T fit the condition with  $N = 3$  and  $N = 2$ , respectively, and thus a  $8e^2/h$ -step appears at  $\bar{\mu} = t$ . We also find that the disappearance of a zero-Hall conductivity plateau is always accompanied by the occurrence of a  $8e^2/h$ -step at  $\bar{\mu} = t$ , because if  $B = \pi t^2/Ne\hbar v_F^2$ ,  $B$  would satisfy  $B = 4\pi t^2/N'\hbar v_F^2$  with  $N' = 4N$ . Interestingly, here we find that the structure of the Hall plateaus of the AA-stacked BLG would be significantly affected by the applied magnetic field, which is quite different from the MLG and the AB-stacked BLG.

#### IV. SUMMARY

In conclusion, we have calculated both the quantized Hall conductivity and longitudinal conductivity of the AA-stacked bilayer graphene within linear response theory by using Kubo formula. We find that the dependence of the Hall plateau of the AA-stacked BLG on the

magnetic field is distinctly different from both the MLG and AB-stacked BLG as well as the conventional quantum Hall materials. In particular, the AA-stacked bilayer graphene could possess the unique  $\bar{\nu} = 0$  plateau, in contrast to other graphene materials such as monolayer and AB-stacked bilayer graphene. The shift of level anomalies due to interlayer hopping energy is attributed to be the origin of the  $\bar{\nu} = 0$  plateau. Nonetheless, the  $\bar{\nu} = 0$  plateau across  $\bar{\mu} = 0$  would disappear if magnetic field  $B = \pi t^2/Ne\hbar v_F^2$ . In addition, we find that the disappearance of a zero-Hall conductivity plateau is always accompanied by the occurrence of a  $8e^2/h$ -step at  $\bar{\mu} = t$ . Furthermore, when  $|\bar{\mu}| = [(\sqrt{n_1} + \sqrt{n_2})/(\sqrt{n_2} - \sqrt{n_1})]t$ , the AA-stacked BLG lacks the  $\bar{\nu} = \pm 4(n_1 + n_2)n$  plateaus, which exist in the AB-stacked BLG. We also find that when  $\Gamma \rightarrow 0$  and  $\hbar^4\omega_c^4 \gg (\bar{\mu} + \nu t)^4$ ,  $\sigma_{xx} \rightarrow 0$  if the Fermi level is not a few  $\Gamma$ s above and below a Dirac point. This implies that at the high magnetic field, the external electric field cannot drive any current for  $\bar{\mu} < t$  while the current would be perpendicular to the external electric field for  $\bar{\mu} > t$ . We hope that our predicted interesting characteristics of quantum Hall effect in the AA-stacked BLG, which are not seen in both the MLG and BLG as well as the conventional quantum Hall materials, would stimulate experimental effort on fabricating the AA-stacked BLG and also on measurement of its transport property in the near future.

#### ACKNOWLEDGEMENTS

The authors thank Hung-Yu Yeh, Tsung-Wei Chen and Ming-Che Chang for valuable discussions. The authors also acknowledge financial supports from National Science Council and NCTS of Taiwan.

- 
- [1] A. H. Castro Neto, N. M. R. Peres, K. S. Novoselov, and A. K. Geim, *Rev. Mod. Phys.* **81**, 109 (2009).
  - [2] P. R. Wallace, *Phys. Rev.* **71**, 622 (1947)
  - [3] M. I. Katsnelson, K. S. Novoselov, And A. K. Geim, *Nat. Phys.* **2**, 620 (2006).
  - [4] V.P. Gusynin, and S.G. Sharapov, *Phys. Rev. Lett.* **95**, 146801 (2005).
  - [5] K. S. Novoselov, A. K. Geim, S. V. Morozov, D. Jiang, M. I. Katsnelson, I. V. Grigorieva, S. V. Dubonos and A. A. Firsov, *Nature (London)* **438**, 197 (2005).
  - [6] Y. Zhang, Y. W. Tan, H. L. Stormer, and P. Kim, *Nature (London)* **438**, 201 (2005).
  - [7] K.S. Novoselov, Z. Jiang, Y. Zhang, S. V. Morozov, H. L. Stormer, U. Zeitler, J. C. Maan, G. S. Boebinger, P. Kim, and A.K. Geim, *Science* **315**, 1379 (2007).
  - [8] E. McCann and V. I. Fal'ko, *Phys. Rev. Lett.* **96**, 086805 (2006).
  - [9] K. S. Novoselov, E. McCann, S. V. Morozov, V. I. Fal'ko, M. I. Katsnelson, U. Zeitler, D. Jiang, F. Schedin and A. K. Geim, *Nat. Phys.* **2**, 177 (2006).
  - [10] M. Nakamura, L. Hirasawa, and K.-I. Imura, *Phys. Rev. B* **78**, 033403 (2008).
  - [11] M. Aoki and H. Amawashi, *Solid State Commun.* **142**, 123(2007).
  - [12] P. L. de Andres, R. Ramırez, and J. A. Verges, *Phys. Rev. B* **77**, 045403 (2008).
  - [13] P. Lauffer, K. V. Emtsev, R. Graupner, Th. Seyller, and L. Ley, *Phys. Rev. B* **77**, 155426 (2006).
  - [14] Z. Liu, K. Suenagam, H. Suzuura, P. J. F. Harris, and S. Iijima, *Phys. Rev. Lett.* **102**, 015501 (2009).
  - [15] H. Bruus, and K. Flensberg, *Many-Body Quantum Theory in Condensed Matter Physics* (Oxford, New York, 2007), Chaps. 6 and 11.
  - [16] G. D. Mahan, *Many-Particle Physics* (Plenum Press, New York, 2000), Chap. 4.
  - [17] M. Iwasaki, H. Ohnishi and T. Fukutome, *J. Phys. G: Nucl. Part. Phys.* **35**, 035003 (2008).
  - [18] A. Endo, N. Hatano, H. Nakamura, and R. Shirasaki, *J. Phys. : Condens. Matter* **21**, 345803 (2009).
  - [19] N. N. Lebedev, *Special Functions and Their Applications*

- (Dover, New York, 1972), Chap. 1.
- [20] V. P. Gusynin, and S. G. Sharapov, *Phys. Rev. B* **71**, 125124 (1972).
- [21] H. Y. Yeh (private communication).
- [22] M. Janßen, O. Veihweger, U. Fastenrath, and J. Hajdu, *Introduction to the Theory of the Integer Quantum Hall Effect* (VCH, Weinheim, 1994).
- [23] D. Yoshioka, *The Quantum Hall effect* (Spring-Verlag, Berlin Heidelberg, 2002), Chap. 7.
- [24] E. H. Hwang, S. Adam, and S. Das Sarma, *Phys. Rev. Lett.* **98**, 186806 (2007).
- [25] J. Martin, N. Akerman, G. Ulbricht, T. Lohmann, J. H. Smet, K. Von Klitzing, and A. Yacoby, *Nat. Phys.* **4**, 144 (2008).
- [26] Y. F. Hsu, and G. Y. Guo, *Phys. Rev. B* **81**, 045412 (2010).
- [27] A. K. Geim, *Science* **324**, 1530 (2004).
- [28] L. Zhang, Y. Zhang, M. Khodas, T. Valla, and I. A. Zaliznyak, *arXiv:1003.2738* (2010).